

Convergence of force calculations for noncrystalline Si

D. A. Drabold and J. D. Dow

Department of Physics, University of Notre Dame, Notre Dame, Indiana 46556

P. A. Fedders and A. E. Carlsson

Department of Physics, Washington University, Saint Louis, Missouri 63130

Otto F. Sankey

Department of Physics, Arizona State University, Tempe, Arizona 85287

(Received 16 January 1990; revised manuscript received 1 May 1990)

We compare the forces generated by various angle-dependent potentials and by *ab initio* band-structure calculations with a limited number of \mathbf{k} points. In cells with 32 and 54 atoms we find substantial errors for all of the angle-dependent-force models, as well as for the band-structure forces with very few \mathbf{k} points.

Recently there have been a number of computer simulations of amorphous solid Si (*a*-Si) and of liquid Si (*l*-Si) using two distinct methods: (i) empirically fitted angle-dependent forces (ADF) (Refs. 1–8), and (ii) first-principles band-structure-derived forces (BSF).^{9,10} Finite Si clusters and reconstructed Si surfaces have also been studied. Similar studies have been performed or are being performed for other materials.¹¹ Both of these methods, ADF and BSF, have inaccuracies that have not been systematically evaluated for liquid and amorphous geometries. The ADF models are fit to a fairly small database so that one might question how well they predict the forces in an amorphous solid or liquid. This is especially true since relatively small errors in total energies can lead to rather large errors in forces. The BSF methods, which use first-principles molecular-dynamics simulations within a supercell geometry are not fit. However, because of the computational complexity in actually implementing them, they have a different set of difficulties. One can ask how important cell size is and/or what the dependence is on the band curvature or number of \mathbf{k} points in the Brillouin zone. In this communication, we briefly investigate these questions. For the ADF models we have limited our investigations to the potentials of Stillinger and Weber (SW),¹ the two potentials of Biswas and Hamann [BH-1 (Ref. 5) and BH-2 (Ref. 6)], and the model of Carlsson, Fedders, and Myles (CFM).⁷ Concerning the BSF method, the cell size and \mathbf{k} -point sampling were investigated using the *ab initio* total-energy–molecular-dynamics scheme of Sankey and Niklewski.¹²

For the BSF model, we find that the use of only the Γ ($\mathbf{k}=\mathbf{0}$) point in samples of from 32 to 54 atoms leads to typical errors of 0.3–0.4 eV/Å. These are small in comparison with typical force scales in Si that are of order several eV/Å. However, errors of this magnitude caused one sample to remain amorphous upon annealing, when a more accurate calculation led to crystallization. Further, we have generally found fewer defects in samples annealed with a more accurate procedure. This suggests that the energy barriers (or necessary forces) for crystallization and defect healing are much lower than the natural scale in Si. Increasing the number of points to eight can still lead to non-negligible error. The ADF models all yield errors several times larger than the Γ -point BSF

method.

We first examine the accuracy of the BSF method. *Ab initio* molecular-dynamics simulations usually involve the use of “supercells,” because it is computationally impossible to simulate a cluster large enough to ignore surface states. In addition, supercells are convenient since it is quite straightforward to use the apparatus of crystalline solids to simulate approximately an infinite system. One chooses a particular Bravais lattice with a large unit cell, and periodically repeats the cell through all space. The aim of this construction is to eliminate spurious surface effects, while providing a cell large enough to include a representative sample of local microstructures. The properties of this infinite system are then easily handled with \mathbf{k} -space methods. A crucial aspect of this procedure is the choice of geometry of the cell.

If the supercell is large enough so that intercell interactions are negligible, we are still left with the requirement of handling the “supercell bands” properly. Because the supercell lattice constant is much larger than typical interatomic spacings, the supercell bands are much narrower than for a system with a smaller unit cell. In this paper we examine the effects of curvature and dispersion of the supercell bands on the atomic forces, in some commonly used supercell geometries. The systems we treat are disordered and have a finite electronic density of states at the Fermi level. The Fermi level’s crossing the supercell bands is expected to enhance the effects of the band dispersion on the total energy. If all bands were completely filled or empty, then only the center of gravity of a band, and not its width, would affect the total energy. This is not true for partially filled bands. Typical ADF methods yield 15% or more defects, which yields a sizable density of states at the Fermi level.

It has become a common practice in *ab initio* molecular-dynamics simulations to use one \mathbf{k} point in the Brillouin zone to calculate energies and forces. In effect this assumes that the supercell bands are flat. For computational reasons, the Γ point ($\mathbf{k}=\mathbf{0}$) is usually selected for this purpose. To evaluate this procedure, we have calculated the supercell bands for a 54-atom fcc structure that is highly disordered. There is significant dispersion in the bands for the 54-atom cell, with widths of order 0.1 eV. We performed a similar calculation for the 54-atom

cell in the diamond structure, and see comparable dispersion. We will show that the Γ -point sampling scheme can lead to serious errors in interatomic forces. To demonstrate this, we perform calculations that are in all respect identical except for how sums over the BZ are performed: we compare the Γ -point results with the results of using four or sixteen Monkhorst-Pack¹³ special points, which yields eight or thirty-two points in the BZ. If one uses an ADF model one can easily calculate with supercells that are large enough so that size is not a problem. We consider four different types of ADF schemes. The first of these, developed by Stillinger and Weber¹ (SW), aims to obtain the simplest possible description of the energies that yields both a stable diamond structure and reasonable liquid properties. The SW energy functional has the form of an interatomic potential series with two- and three-body terms. The two-body term is a short-ranged pair potential cut off inside the second-neighbor distance and the three-body potential has the form

$$V_3(R_i, R_j, R_k) = Cf(R_{ij})f(R_{ik})(\cos\theta_{jik} + \frac{1}{3})^2. \quad (1)$$

Here, f is a radial function with the same cutoff as V_2 , and θ_{jik} is the angle at atom i subtended by atoms j and k . The form of the angular term is such that it vanishes for the diamond structure but is positive for plausible competing structures. The functional has seven adjustable parameters, whose values were obtained by insisting that the melting point and the radial distribution function of the liquid be obtained reasonably well.

Biswas and Hamann (BH) have generated two types of two- and three-body potential schemes for Si. The first, BH-1,⁵ was designed to treat structural energy differences, which are not obtained well by potentials as simple as that of SW. The potentials are longer ranged than those of SW and have a more complicated angular variation. The pair potential V_2 has an exponential decay and calculations typically retain interactions up to 10 Å. The three-body potential has the separable form

$$V_3(R_i, R_j, R_k) = \sum_{l=1}^6 C_l f_l(R_{ij})f_l(R_{ik})P_l(\cos\theta_{jik}), \quad (2)$$

where the f_l are exponential decay functions and the P_l are the Legendre polynomials. The model has fourteen adjustable parameters, which are fit to a database of volume-dependent structural-energy differences obtained from *ab initio* calculations, as well as the energy of a four-layer slab. Despite the long range of the energy functional, it is practical to perform large-scale atomistic simulations by the use of “structural moments,” which allow the three-body term to be evaluated by computing only two-body terms.⁵

The BH-2 functional⁶ is designed to treat properties of bonding defects, such as surfaces, vacancies, and interstitials. It has the same functional form as the BH-1 potential, but with a more rapid radial decay. In addition, only terms in Eq. (2) with $l \leq 2$ are included. The model contains eight adjustable parameters, which were fitted to both bulk structural energy differences and an enlarged collection of defect properties, with emphasis on the latter.

The last ADF scheme we treat was developed by

Carlsson, Fedders, and Myles⁷ (CFM). It generalizes the “embedded-atom” format to obtain angular forces, and includes environmental effects on the effective interatomic potentials. The aim is to provide a rudimentary description of both bonding defects and structural energies. The CFM energy functional has the following form:

$$E = \frac{1}{2} \sum V_2^{\text{rep}}(R_i, R_j) + \sum [E_{\text{el}}^{(2)}(i) + E_{\text{dip}}(i) + E_{\text{el}}^{(4)}(i)]. \quad (3)$$

Here, V_2^{rep} is a short-ranged repulsive pair potential. The $E_{\text{el}}^{(2)}$ and E_{dip} terms are obtained from the “second-moment” matrix $\hat{\mu}_2(i)$, which contains information about the radial and angular distribution of the neighbors of atom i ; this matrix is given as a sum of pair terms. The electronic $\hat{\mu}_2$ term is given by $E_{\text{el}}^{(2)}(i) = -\text{Tr}[\hat{\mu}_2(i)]^{1/2}$, and $E_{\text{dip}}(i)$ describes the asymmetry of the local environment as given by the s - p part of $\hat{\mu}_2(i)$. Finally, $E_{\text{el}}^{(4)}(i)$ is a sum of three- and four-body path terms, multiplied by an environmental factor. The functional contains eight adjustable parameters, whose values were obtained by fitting to a database including *ab initio* structural energy differences, elastic constants, and the vacancy-formation energy.

We have made comparisons between methods on a number of samples but our results are well characterized by just two samples.¹⁴ Sample *A* (for amorphous) contains 32 atoms in a bcc unit cell, while sample *L* (for liquid) contains 54 atoms in a fcc unit cell. Both samples have the density of *a*-Si. The initial state in producing sample *A* was a crystal solid melted at 6000 K. The procedure for removing energy from the system was to allow the sample to evolve at constant total energy until it reached a minimum in the potential energy. At this point the kinetic energy was set equal to zero, and the sample was allowed to evolve at constant energy until it reached the next potential-energy minimum. This process was repeated until the kinetic energy at the potential energy minimum was less than 10 K, which required 30–40 repetitions, depending upon the initial liquid configuration. The evolution from one potential-energy minimum to the next typically required 15–20 time steps of 10^{-15} sec. Although *a*-Si has never been made in the laboratory from liquid Si, the radial distribution function of sample *A*, shown in Fig. 1, is similar to that of *a*-Si.^{15,16} We note that no simulation has come close to reproducing typical laboratory condition for making *a*-Si. Further, because of the necessity of short time steps, it is unlikely that anyone will simulate laboratory conditions in the near future. However, we also note that various methods of growing *a*-Si yield virtually identical samples. The sample contains two dangling bonds (three-fold-coordinated atoms), where coordination is defined by a radius of 2.7 Å. The rest of the atoms are fourfold coordinated. Further, about $\frac{1}{3}$ of the rings in this sample were of 5 or 7 members instead of the 6 for a crystal. The bond angles ranged from 74° to 167°, but 90% of the bond angles were within a 29° spread about 109°, and 80% of them were within a 23° spread. Starting with this near equilibrium sample, we began further annealing using only the Γ point with the BSF program. It reached equilibrium as an amorphous sample with the same two defects. How-

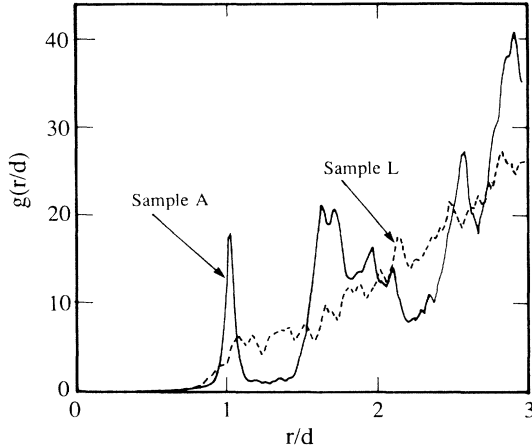


FIG. 1. Radial distribution function of samples *A* and *L* in reduced units of $d=2.35$ Å.

ever, starting with the same near equilibrium sample, when it was annealed further with four \mathbf{k} points, it became a crystal. Thus, the structures that emerge are very sensitive to the interatomic forces. Although (as mentioned above) the annealing sequence that was used is certainly far removed from the actual physical growth process for *a*-Si, we see no reason why the physical growth process should be less sensitive to the forces. Sample *L* was obtained in the same fashion as sample *A*, but the procedure was stopped when the kinetic energy was still several thousand degrees per atom. Its radial distribution function is shown in Fig. 1, and is basically liquid-like. However, the radial distribution function is quite different from the experimental one.¹⁷ This is not a serious problem, since these samples were created in order to test the potentials and not to simulate real *l*-Si. Thus our two samples include a sample that is close to being *a*-Si and a sample that is still quite liquid-like. Our results on the forces are summarized in Table I (for the 32-atom sample *A*) and Table II (for the 54-atom sample *L*). We have defined ΔF as a root-mean-square deviation

$$\Delta F = \left[N^{-1} \sum_i [\mathbf{F}(i) - \mathbf{F}_e(i)]^2 \right]^{1/2},$$

where $\mathbf{F}(i)$ is the computed force on atom i , $\mathbf{F}_e(i)$ is the exact (16-point BSF method) force on atom i , and N is the number of atoms (32 or 54). The quantities $\delta_i F$ in the tables are the errors in the forces for the 3 or 5 worst atoms. The quantity $\Delta F'$ is the same as ΔF except that the worst 10% of the atoms were taken out of the sum and thus N is 29 or 49. The rms force on the atoms in

sample *A* is 0.35 eV/Å and in sample *L* is 4.9 eV/Å.

Since sample *A* had been extensively annealed, the exact forces are small and thus the relative error in the forces is rather large compared to the rms total force. It is interesting to note the atoms on which the errors were the greatest are highly correlated not only among the various ADF methods but also between the ADF methods and the Γ -point BSF method. For this reason atom numbers of the worst atom are included in parentheses in Tables I and II. Atoms no. 12, 24, and 29 all have one bond angle of less than 90° , atom no. 31 has bond angles between 96° and 127° , and atom no. 9 has a dangling bond. Evidently almost all of the methods have more trouble with badly strained bonds than with dangling bonds. Further, from the tables, one can see that a substantial part of the rms error comes from 10% of the atoms.

For the 54-atom more-liquid-like sample *L*, we note that all of the ADF methods predict forces that are in error by about the magnitude of the exact forces, while the BSF method is much better, even with one \mathbf{k} point. Since we have found no correlations between the methods on which atoms were treated worst, we have not included the atom numbers in this case. We have also noted some dynamical differences between the methods. For example, if one plots $r^2(t)$ versus t with the exact BSF method, one obtains a reasonably straight line indicating the expected diffusive behavior. However, with only one \mathbf{k} point, r^2 is supralinear, suggesting a partially ballistic behavior.

Some further general trends are evident as one goes from the least-accurate methods (the ADF models) to Γ -point BSF calculations and finally to exact BSF calculations. One trend that is evident among all of the methods is that more accurate methods tend to favor crystals and methods with larger errors tend to favor disorder. As noted earlier, we found samples that had converged to an amorphous sample using the Γ -point BSF method but that became crystalline when annealed further with more \mathbf{k} points. Further, it has become clear from other investigations¹⁸⁻²¹ that the ADF methods invariably give very large (or order 15–20%) concentrations of defects. Another trend is evident on a shorter time scale. This is the observation that distortions from perfect crystal or from tetrahedral coordination are relaxed faster and more completely with the better methods.

In order to understand better the origins of the errors caused by using a finite number of \mathbf{k} points, we have performed some additional calculations. It is well known

TABLE I. Comparison of the errors in the 32-atom cluster, sample *A*. The root-mean-square error ΔF is defined in the text and $\delta_i F$ are the errors in the forces for the worst three atoms. The numbers in parentheses refer to the one atom number in the cluster and all units are eV/Å.

Method	ΔF	$\Delta F'$	$\delta_1 F$	$\delta_2 F$	$\delta_3 F$
BS ($\mathbf{k}=0$)	0.34	0.23	0.74(12)	0.62(21)	0.54(29)
BH-1	1.54	1.41	2.80(9)	2.27(29)	2.25(19)
BH-2	0.74	0.57	2.06(12)	1.49(31)	1.28(29)
SW	1.09	0.66	3.13(31)	3.12(18)	2.48(12)
CFM	1.01	0.81	2.43(12)	2.077(31)	1.84(24)

TABLE II. Errors in the forces for the 54-atom cluster, sample *L*. The root-mean-square error ΔF is defined in the text and $\delta_i F$ are the errors in the forces for the worst five atoms. All units are eV/Å.

Method	ΔF	$\Delta F'$	$\delta_1 F$	$\delta_2 F$	$\delta_3 F$	$\delta_4 F$	$\delta_5 F$
BS (4 \mathbf{k} points)	0.15	0.14	0.24	0.23	0.20	0.20	0.20
BS($k=0$)	0.43	0.39	0.83	0.80	0.74	0.72	0.68
BH-1	15.54	7.48	65.65	61.41	31.38	30.63	17.11
BH-2	2.45	2.19	4.40	4.40	4.39	4.09	3.85
SW	4.01	3.52	8.45	7.95	6.91	6.40	6.34
CFM	6.98	4.54	25.69	23.99	12.96	10.97	9.99

that in order to obtain accurate Brillouin-zone (BZ) integrations, one needs more \mathbf{k} points for materials with a finite density of states at the Fermi energy than for materials with a gap at the Fermi energy. To establish the importance of this effect, we performed calculations for the energies and forces on crystals that were allowed to disorder slightly by small random motions. In case I we allowed rms excursions of roughly 0.1 Å. This sample retained a gap of about 1 eV. In case II we allowed rms excursions of roughly 0.2 Å, and the gap barely closed. Both samples contained 54 atoms. In both cases the error obtained by using only one \mathbf{k} points was 0.26 eV per atom. However, the rms error in the force in case I was 0.13 eV/Å, while the error was 0.53 eV/Å in case II. This suggests that the majority of the error is in the bands crossing the Fermi surface. Further, we note that the energy differences between different crystal structures are often less than 0.26 eV per atom.

One can understand this result in the following way. We view the use of different numbers of \mathbf{k} points in the BZ as corresponding to different interpolations for $E(\mathbf{k})$ versus \mathbf{k} between the chosen \mathbf{k} points. The approximate $E(\mathbf{k})$ then oscillates about the exact $E(\mathbf{k})$ over a distance $\Delta\mathbf{k}$ in \mathbf{k} space and with an amplitude proportional to $\Delta\mathbf{k}$. For bands crossing the Fermi surface the integral is cut short, leading to errors of order $(\Delta\mathbf{k})^2$ (a length times a height). The first factor of $\Delta\mathbf{k}$ comes from the number of wave functions that are affected, and the second one comes from the distance of these wave functions from the Fermi level. On the other hand, the error in the charge

density, which determines the electric field and thus the forces, is of order $\Delta\mathbf{k}$. Thus the total energy is in error by terms of order $(\Delta\mathbf{k})^2$, while the forces are in error by terms that are linear in $\Delta\mathbf{k}$.

In conclusion, we have shown that the ADF methods studied yield forces for badly disordered samples far from equilibrium that are in error by about the magnitude of the forces. In terms of absolute error, these methods are much better for samples that are nearer to equilibrium but are still only qualitatively correct. Whether they can yield reliable defect or surface structures is open to question. The Γ -point BSF method for small clusters is worst when far from equilibrium. For such clusters the forces are in error by about 0.4 eV/Å and in error by about 0.1–0.2 eV/Å when using four \mathbf{k} points. The absolute error in the forces when using only one \mathbf{k} point is rather small for nearly converged samples, but this small error can make the difference between an amorphous and crystalline sample.

This work was supported in part by the Office of Naval Research (ONR), U.S. Department of Defense, under Grants No. N00014-90-J-1304 and N-00014-84-K-03552, by the National Science Foundation (NSF) under Grant No. DMR-88-01260, the U.S. Department of Energy under Grant No. DE-FG02-84ER45130, and by the Solar Energy Research Institute (SERI) under Subcontract No. XB-7-06055-1 of Contract No. DE-AC02-83CH10093. We wish to acknowledge considerable help from Stefan Klemm.

¹F. H. Stillinger and T. A. Weber, Phys. Rev. B **31**, 5202 (1985).

²J. Tersoff, Phys. Rev. Lett. **56**, 632 (1986); Phys. Rev. B **37**, 6991 (1988).

³M. I. Baskes, Phys. Rev. Lett. **59**, 2666 (1988).

⁴M. I. Baskes, J. S. Nelson, and A. F. Wright, Phys. Rev. B **40**, 6085 (1989).

⁵R. Biswas and D. R. Hamann, Phys. Rev. Lett. **55**, 2001 (1985).

⁶R. Biswas and D. R. Hamann, Phys. Rev. B **36**, 6434 (1987).

⁷A. E. Carlsson, P. A. Fedders, and C. W. Myles, Phys. Rev. B **41**, 1247 (1990).

⁸A. E. Carlsson, in *Solid State Physics: Advances in Research and Applications*, edited by H. Ehrenreich and D. Turnbull (Academic, New York, 1990), Vol. 43, p. 1.

⁹I. Štich, R. Car, and M. Parrinello, Phys. Rev. Lett. **63**, 2240 (1989).

¹⁰R. Car and M. Parrinello, Phys. Rev. Lett. **60**, 204 (1988).

¹¹G. Galli, R. Martin, R. Car, and M. Parrinello, Phys. Rev. Lett. **62**, 555 (1989).

¹²O. F. Sankey and D. J. Niklewski, Phys. Rev. B **40**, 3979

(1989).

¹³H. J. Monkhorst and J. D. Pack, Phys. Rev. B **13**, 5188 (1976).

¹⁴Coordinates and forces for these samples are available upon request.

¹⁵F. Fortner and J. S. Lanin, Phys. Rev. B **39**, 5527 (1989).

¹⁶J. H. Etherington, A. C. Wright, J. T. Wenzel, J. C. Dore, J. H. Clarke, and R. N. Sinclair, J. Non-Cryst. Solids **48**, 265 (1982).

¹⁷J. P. Gabathuler and S. Steeb, Z. Naturforsch. **34A**, 1314 (1979).

¹⁸R. Biswas, I. Kwon, A. M. Bouchard, C. M. Soukoulis, and G. S. Grest, Phys. Rev. B **39**, 5101 (1989); R. Biswas, Gary S. Grest, and C. M. Soukoulis, *ibid.* **38**, 8154 (1988).

¹⁹J. Q. Broughton and X. P. Li, Phys. Rev. B **35**, 9120 (1987).

²⁰M. D. Kluge, J. R. Ray, and A. Rahman, Phys. Rev. B **36**, 4234 (1987).

²¹W. D. Luedtke and U. Landman, Phys. Rev. B **37**, 4656 (1988).